Self-assembled lipid nanostructures encapsulating nanoparticles in aqueous solution

ARTICLE *in* SOFT MATTER · OCTOBER 2009

Impact Factor: 4.03 · DOI: 10.1039/b906918f

Self-assembled lipid nanostructures encapsulating nanoparticles in aqueous solution

Guang-Kui Xu,[a] Yue Li,[a] Bo Li,[a] Xi-Qiao Feng*[a] and Huajian Gao[b]

Received 7th April 2009, Accepted 4th June 2009
First published as an Advance Article on the web 14th July 2009
DOI: 10.1039/b906918f

Liposomes and nanoparticles, as well as their composite nanostructures, have great promise for potential applications in the nanobiotechnology of drug delivery and cancer therapy. Here, we use the self-consistent field method to investigate the interaction between lipid molecules and nanoparticles in an aqueous solution. It is shown that lipid molecules can self-assemble into monolayered or bilayered structures encapsulating nanoparticles. By varying the concentration of lipid molecules as well as the surface charge density and size of particles, several novel self-assembled nanostructures have been found. This method could be used to predict and design novel nanovehicles and nanomedicine carries for various biomedical applications, and the obtained results are helpful for gaining a deeper understanding of lipid-nanoparticle interactions.

Introduction

In the past decade, nanobiotechnology has been exploited as a highly promising area devoted to developing novel nanoscale techniques for disease diagnosis, treatment, and drug delivery.[1–3] Liposomes and polymeric nanoparticles represent two dominant classes of nanomedicine carriers for drug encapsulation and delivery.[4,5] Liposomes are tiny vesicles constructed from amphiphilic lipid molecules. They are biocompatible and capable of storing various drug molecules, and functionalized liposomes can target almost all types of cells in the body. Therefore, they have been accepted as a good candidate for pharmaceutical carriers. For example, hydrophilic pharmaceutical agents can be encapsulated into water compartments of liposomes, whereas hydrophobic pharmaceuticals can be entrapped in the membranes.[6,7] Recently, polymeric nanoparticles, self-assembled by biodegradable copolymers, emerged as another useful tool in the nanomedicine area. Amphiphilic block copolymers in an aqueous solution can self-assemble into a unique core-shell structure (usually 10–100 nm in diameter), in which the hydrophobic core serves as a natural carrier for hydrophobic drugs while the hydrophilic shell plays a stabilizing role.[8–10]

Given the clinical success of nanoparticles and liposomes, nanostructures consisting of one or more lipid layers surrounding a nanoparticle with or without surface charges have been developed recently.[4,11–16] Such self-assembled nanosized systems hold the advantages of both nanoparticles and liposomes. These composite structures have great potential applications in nanomedicine and can be used as a novel and robust drug delivery strategy with favorable features such as high drug encapsulation, continuous drug release, stable incorporation of cancer chemotherapeutic agents, controlled release of two or more drugs for cancer therapy, among others.[4,11,12]

Considerable effort has been directed towards understanding the physical mechanisms of interaction between nanoparticles and vesicles or cell membranes.[17–19] Their interaction involves three main characteristic length dimensions, namely, the particle size, the membrane thickness, and the vesicle size. A particle, considerably smaller than a vesicle but larger than the membrane thickness, can be fully wrapped by a vesicle if their adhesion strength is sufficiently strong.[17] The shortest wrapping time is related to the particle size.[18] Recently, Ginzburg and Balijepalli studied the interaction between a cell membrane and a nanoparticle that is much smaller than the cell size and yet comparable to the membrane thickness.[19] In spite of these studies, there is still a shortage of theoretical investigations on the self-assembly of lipid-nanoparticle structures, which are of both theoretical and technological interest.

As a mesoscopic polymer theory, the self-consistent field theory (SCFT) has been proven to be a powerful method for the study of the ordered phases of block copolymers.[20,21] In this method, local monomer densities and chemical potential fields are used to determine the free energy of the system. SCFT is favorable for analyzing the thermodynamics of copolymers based on mean field representations of the internal energy and entropy. Recently, SCFT has also been extended to explore the aggregation behavior of diblock copolymers in dilute solution.[22,23] Here we employ SCFT to predict self-assembled nanostructures of lipid layers enveloping nanoparticles in an aqueous solution. We will adopt the combinatorial screening technique for solving SCFT equations in real space.[24,25] Since there is no need to make any assumptions about the equilibrium morphology, the method can be used to predict previously unobserved morphologies of the system.

Method

We consider a system consisting of lipid molecules and nanoparticles mixed in an aqueous solution. Each lipid molecule is

[a]*Institute of Biomechanics and Medical Engineering, AML, Department of Engineering Mechanics, Tsinghua University, Beijing 100084, China. E-mail: fengxq@tsinghua.edu.cn; Fax: +86-10-6278 1824; Tel: +86-10-6277 2934*
[b]*Division of Engineering, Brown University, Providence, RI 02912, USA*

treated as a diblock copolymer consisting of distinctly different segments linked together by covalent bonds. The nanoparticle surfaces are assumed to be hydrophobic, motivated by considerations of drugs that are poorly soluble in water. In our calculations, we choose a two-dimensional representative volume element (RVE) to study the interaction between lipid molecules and nanoparticles. The RVE contains only one nanoparticle with radius R_0, embedded in a mixture of diblock copolymers (D) and water (W). The deformation of the nanoparticle is neglected; in other words, the particle is approximated as an external field with a hard wall. Each diblock copolymer is modeled as a flexible Gaussian chain consisting of N total segments with segment volume ρ_0^{-1}, including hydrophobic segments (A) and hydrophilic segments (B). The volume fraction of the A segments per chain is denoted as f. We assume that the A and B segments and water molecules all have the same statistical length a. The volume fractions of diblock copolymers and water in the solution are denoted as φ_D and $\varphi_W = 1 - \varphi_D$, respectively.

Let $\phi_I(\mathbf{r})$ (I = A, B and W) denote, respectively, the local volume fractions of A segments, B segments, and water molecules at position $\mathbf{r}$. We assume that the diblock copolymers cannot penetrate into the nanoparticle; in other words, the copolymers are confined by the nanoparticle surface. With this constraint, the incompressibility condition takes the following form[26,27]

$$\phi_A(\mathbf{r}) + \phi_B(\mathbf{r}) + \phi_W(\mathbf{r}) = \Phi_0(\mathbf{r}) \tag{1}$$

where

$$\Phi_0(\mathbf{r}) = \begin{cases} 0, & r \le R_0 \\ \dfrac{1-\cos[\pi(r-R_0)/\varepsilon]}{2}, & R_0 \le r \le R_0+\varepsilon \\ 1, & r \ge R_0+\varepsilon \end{cases} \tag{2}$$

ensures that the segment density decays smoothly across the solid-liquid interface, defined as a thin layer of thickness ε around the particle surface.

In the SCFT method, the pair interactions between different components are determined by a set of effective chemical potential fields, $W_I(r)$, denoting the magnitude of the mean field felt by the species I at position $\mathbf{r}$. The dimensionless Helmholtz free energy of the system is given by[27,28]

$$F = \frac{NF_0}{\rho_0 k_b T V} = F_D + F_W + F_E \tag{3}$$

where V is the total volume of the solution. The diblock entropic free energy F_D is expressed as

$$F_D = -\varphi_D \ln\left(\frac{Q_D}{V\varphi_D}\right) - \frac{1}{V}\int d\mathbf{r}\left[W_A(\mathbf{r})\phi_A(\mathbf{r}) + W_B(\mathbf{r})\phi_B(\mathbf{r})\right] \tag{4}$$

where Q_D is the partition function of a single chain subject to the fields $W_A(\mathbf{r})$ and $W_B(\mathbf{r})$; F_W accounts for the entropic contribution of water molecules to the free energy and is written as

$$F_W = -N\varphi_W \ln\left(\frac{Q_W}{V\varphi_W}\right) - \frac{1}{V}\int d\mathbf{r}\left[W_W(\mathbf{r})\phi_W(\mathbf{r})\right] \tag{5}$$

where Q_W is the partition function of a water molecule under the effective potential field $W_W(\mathbf{r})$; the term F_E represents the enthalpic interactions, including diblock-diblock, diblock-water, diblock-surface, and water-surface interactions, which is expressed as

$$\begin{aligned} F_E = \frac{1}{V}\int d\mathbf{r}\ & \left[N\chi_{AB}\phi_A(\mathbf{r})\phi_B(\mathbf{r}) + N\chi_{AW}\phi_A(\mathbf{r})\phi_W(\mathbf{r})\right. \\ & \left. + N\chi_{BW}\phi_B(\mathbf{r})\phi_W(\mathbf{r})\right] - \frac{1}{V}\int d\mathbf{r}\left[NH_A(\mathbf{r})\phi_A(\mathbf{r})\right. \\ & \left. + NH_B(\mathbf{r})\phi_B(\mathbf{r}) + NH_W(\mathbf{r})\phi_W(\mathbf{r})\right] \end{aligned} \tag{6}$$

where χ_{IJ} is the Flory-Huggins interaction parameter between species I and J. Here $H_I(\mathbf{r})$ describes the surface fields of the nanoparticle for the species I, given by

$$H_I(\mathbf{r}) = \begin{cases} -\infty, & r \le R_0 \\ \dfrac{\Lambda_I}{\varepsilon}\left\{1-\cos[\pi(r-R_0)/\varepsilon]\right\}, & R_0 \le r \le R_0+\varepsilon \\ 0, & r \ge R_0+\varepsilon \end{cases} \tag{7}$$

where Λ_I represents the intensity of the interaction between the particle surface and the species I. A negative and positive value of Λ_I corresponds to repulsive and attractive interaction, respectively.[26,27]

Our numerical calculations are performed in a two-dimensional 256×256 square lattice. Periodic boundary conditions are specified in the axial directions. All length parameters are normalized by the diblock radius of gyration $R_g = a\sqrt{N/6}$. To obtain an equilibrium structure, we minimize the free energy by using the combinatorial screening technique of Drolet and Fredrickson[24,25] implemented with a highly stable and accurate numerical algorithm.[29,30] As noticed by He *et al.*,[22] the resulting aggregation morphology depends, to a certain extent, on the initial fluctuation amplitudes of each species in the dilute solution. In our simulations, the initial fluctuation amplitudes of each species are set as 0.0001 with a random uniform distribution to ensure that the obtained results are almost independent of the initial conditions.[23] The system is thought to have reached equilibrium when the phase patterns become stable and the relative difference of free energy between two neighboring iteration steps is smaller than 0.01%. Furthermore, in each situation, we repeat the simulations for many times using different random numbers in order to guarantee that the self-assembled structures are not accidental. More details on the numerical implementation of SCFT can be found in ref. 19, 29 and 30.

Results and discussions

In this paper, our attention is mainly focused on effects of the content of lipid molecules, the surface properties and sizes of nanoparticles on the self-assembled composite nanostructures. The particle size considered here is much larger than the thickness of vesicles and about tens of nanometers. This range of particle sizes is of practical interest for the application of nanomedicine encapsulation, which is different from the recent study of Ginzburg and Balijepalli[19] who considered nanoparticles with sizes comparable to cell membrane thickness. The volume fraction of nanoparticles in the system is fixed in our simulations. Unless stated otherwise, the normalized length of the simulation box is taken to be $L = 80$, and the normalized radius of the

nanoparticle is set as $R_0 = 15$. The hydrophobic tail and hydrophilic headgroup of a lipid molecule are modeled as A- and B-blocks, respectively. In eqn (2) and (3), the following representative values are used: $\chi_{AB} = 1.0$, $\chi_{AW} = 1.2$, $\chi_{BW} = -0.8$, $f = 0.88$, $N = 25$, and $\varepsilon = 0.65$. To model the hydrophobic particle, we set $\Lambda_A = 0.5$ and $\Lambda_W = -0.75$ in all simulations such that its surface has an attractive interaction with A-blocks and a repulsive interaction with water molecules, while Λ_B is varied from -0.75 to 3.75 in order to account for the effect of the surface charges. For uncharged particles, Λ_B takes a negative value, indicating a repulsive interaction with B-blocks, while for charged particles, Λ_B has a positive value, mimicking an attractive interaction with B-blocks due to electrostatic attraction. Because of the intrinsic complexity of the electrostatic interaction between charged particles and lipid molecules as well as the relatively large size of the calculation model in the present study, we use the parameter Λ_B to describe the intensity of interaction in a phenomenon-based manner. Our simulations will demonstrate that this approach can well predict the formation of various self-assembled composite structures from liposomes and nanoparticles.

We first consider uncharged nanoparticles. In this case, the hydrophobic force plays a predominant role in the self-assembly process. The aggregation morphologies of the water, A- and B-blocks are shown in Fig. 1a. It is seen that lipid molecules form a monolayer surrounding the particle, with the hydrophobic tails pointing to the nanoparticle and the hydrophilic headgroups pointing outward. To reveal the detailed structure, the density profiles of all the species are plotted in Fig. 1b. The hydrophilic B-block density profile in the radial direction has only one maximum value from the particle center to the boundary. Our simulations reveal that an uncharged nanoparticle is generally enveloped by a self-assembled lipid monolayer. Due to the hydrophobic effect, the particle attracts the hydrophobic tails but repels the hydrophilic headgroups and water molecules. Thus, the formation of a self-assembled lipid monolayer around the particle reduces the enthalpic contribution to the free energy. Such a monolayered lipid-nanoparticle structure has been observed in experiments recently.[4,11]

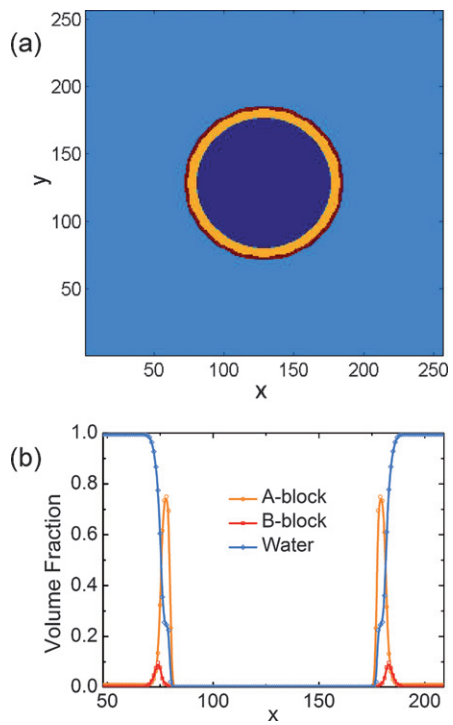

Fig. 1 Density distributions of lipid molecules in the aqueous solution under $\varphi_D = 0.03$ and $\Lambda_B = -0.75$. (a) Aggregation morphologies of A-blocks (orange), B-blocks (red) and water molecules (cyan) around an uncharged nanoparticle (blue). (b) Density profiles of A-blocks (orange), B-blocks (red) and water molecules (cyan) in the radial direction.

If the particle and lipid molecules have the same type of electric charges (either positive or negative), both electrostatic and hydrophobic interactions repel the headgroups of lipid molecules, and our simulations show that only the monolayered lipid nanostructure can form, just as that in the case of uncharged nanoparticles. In what follows, therefore, we mainly study the situation where the particle and lipid molecules have opposite charges. The self-assembled nanostructures are shown in Fig. 2a, c and e under three representative volume fractions of lipid molecules, and the corresponding density profiles are respectively plotted in Fig. 2b, d and f. Fig. 2a shows that at a low volume fraction ($\varphi_D = 0.05$), lipid molecules can self-assemble into a single bilayer structure enwrapping the particle. There are two peaks in the radial density profile of B-block (Fig. 2b). This profile also suggests that the particle is surrounded by a single lipid bilayer resembling a cell membrane. In the self-assembled structure, the headgroups face toward the particle in the inner leaf of the bilayer but face toward water in the outer leaf of the bilayer. In this case, the particle strongly attracts the headgroups due to electrostatic attraction. The attractive force can dominate the hydrophobic force and drive the headgroups together with the particle, leading to the formation of a lipid bilayer. This nanostructure, assembled by oppositely charged nanoparticles and lipid molecules, concurs with De Miguel *et al.*'s experimental observation.[14]

The effect of the concentration of lipid molecules in the solution is also addressed in our study. With increasing concentration, one can obtain self-assembled lipid nanostructures consisting of a single bilayer, two and even three bilayers enveloping the charged nanoparticle, as shown in Fig. 2a, c and e. Correspondingly, the radial density profiles of B-block exhibit two, four and six peaks, respectively (Fig. 2b, d and f). These results clearly reveal that multilayered lipid-nanoparticle structures can be created by increasing the volume fraction of the lipid molecules. Up to now, there have been few experimental reports on such multilayered lipid-nanoparticle structures. Very recently, Bershteyn *et al.*[13] observed similar structures by using an emulsion-solvent evaporation method with a high lipid molecule/copolymer weight ratio. Our study suggests a possible route for the production of nanoparticles encapsulated by multilayered lipid nanostructures. Such special structures may find some significant applications in drug delivery and cancer targeting, although their biophysical properties have not been identified clearly. In practice, multilayered microparticles have already been utilized to substantially prolong the release time of the encapsulated drug.[31–33]

Additionally, one can also see from Fig. 2c and e that the excess lipid molecules outside the lipid layers can self-assemble

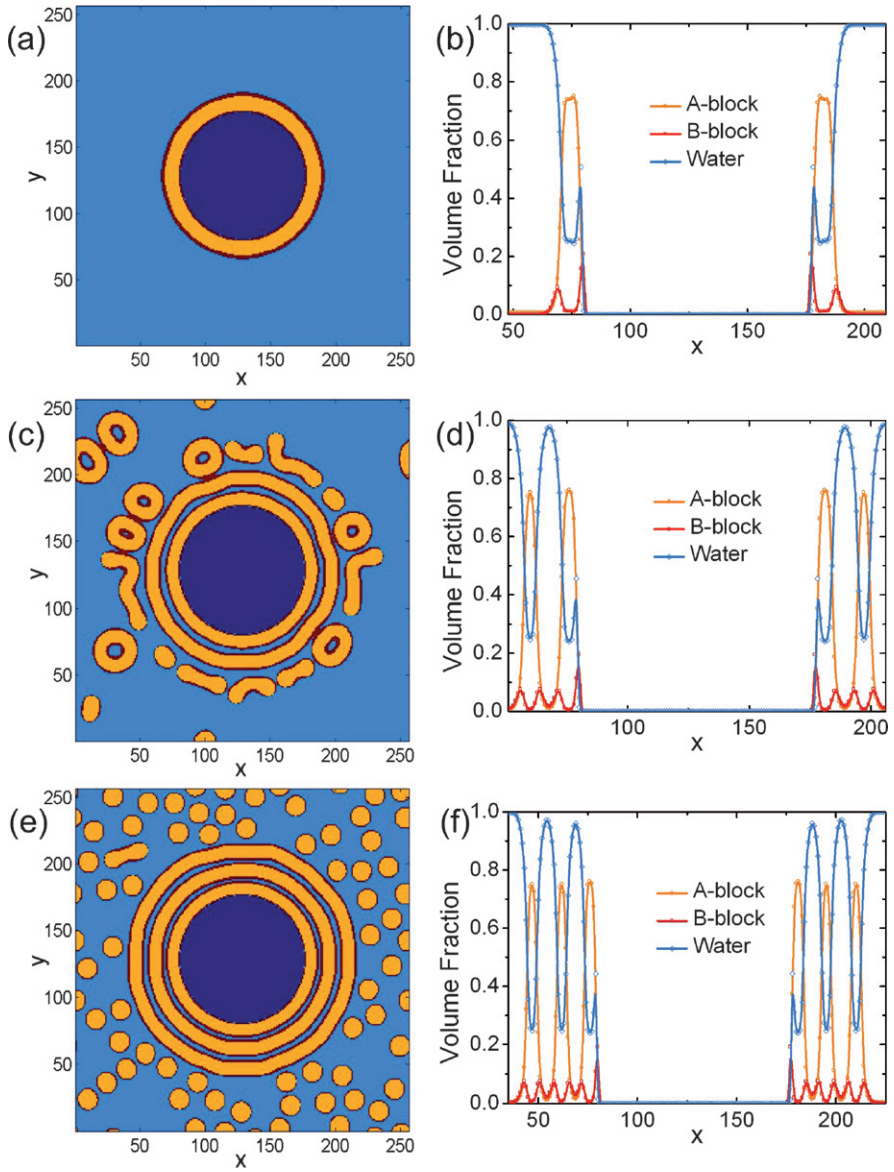

Fig. 2 The influence of the concentration φ_D of lipid molecules on the aggregation morphologies and density profiles of A-blocks (orange), B-blocks (red) and water molecules (cyan) around a charged nanoparticle (blue), where we take $\Lambda_B = 1.75$ and (a and b) $\varphi_D = 0.05$, (c and d) $\varphi_D = 0.15$, and (e and f) $\varphi_D = 0.2$.

into tiny vesicles or micelles of various shapes such as spheres or rods, similar to those simulated in an aqueous solution without particles.[22] The formation of these tiny vesicles far from the nanoparticle seems to be less disturbed by its presence. This is because the electrostatic interaction force decays rapidly due to the formation of the lipid layers surrounding the nanoparticle. In other words, the lipid layers shield the effect of surface charges beyond a limited distance. It appears that no more than three bilayers of lipid molecules can be self-assembled to enwrap the particle even though there are still excess lipid molecules in the solution.

It is interesting to note that the concentric layered structures surrounding a nanoparticle are somewhat similar to the parallel layers found in confined copolymers.[34] For example, when block copolymers are confined in the narrow spacing of two parallel walls, the copolymers may self-assemble into a layered structure parallel to the wall surfaces.[34] The formations of the two types of layered structures are due to the selective interaction between the particle/wall surface and one component of the diblock copolymers, and they both yield a reduction of the free energy of the whole system.

To further examine the effect of surface charge density, we vary the value of the interaction parameter Λ_B in the range from -0.75 to 3.75 under a fixed volume fraction of lipid molecules, $\varphi_D = 0.15$. A larger value of Λ_B indicates a larger surface charge density and results in a stronger attraction between the particle and headgroups. The aggregation morphologies are summarized in Fig. 3 with respect to increasing surface charge density. The uncharged particle is covered by a monolayer and a bilayer of lipid molecules, as shown in Fig. 3a, where we take $\Lambda_B = -0.75$. For a weakly charged particle (*e.g.*, $\Lambda_B = 1.25$), two lipid bilayers can form around the particle (Fig. 3b). With a further increase in

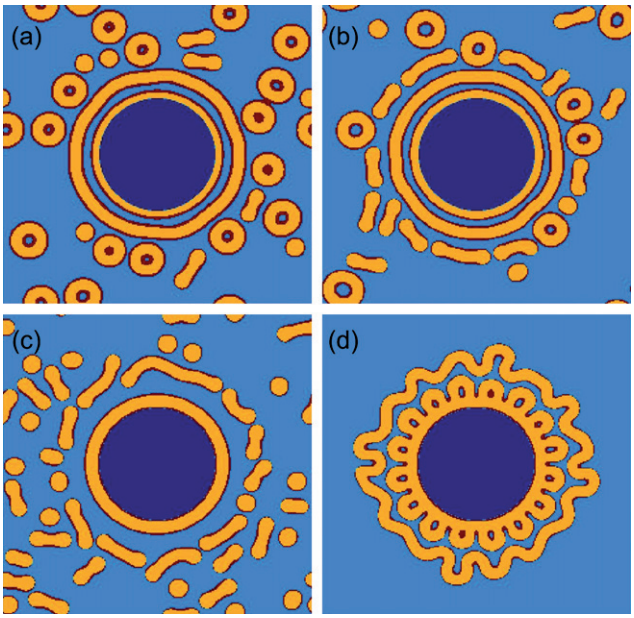

Fig. 3 Aggregation morphologies of A-blocks (orange), B-blocks (red) and water molecules (cyan) around a nanoparticle (blue) under several representative values of the charge density on the particle surface: (a) $\Lambda_B = -0.75$, (b) $\Lambda_B = 1.25$, (c) $\Lambda_B = 2.75$, and (d) $\Lambda_B = 3.75$.

the charge density, the enhanced electrostatic interaction will attract the lipid molecules to form a highly dense bilayer, as shown in Fig. 3c, where $\Lambda_B = 2.75$. In Fig. 3a, b and c, there exist sphere-like or rod-like tiny micelles and vesicles outside the lipid layers owing to their shielding effect to the electric field of surface charges on the particle. For a larger charge density (*e.g.*, $\Lambda_B = 3.75$), more interestingly, a more complex nanostructure is observed, as shown in Fig. 3d. In this case, the lipid layers cannot fully shield the strong interaction induced by the surface charges of the nanoparticle, and the strong electrostatic interaction attracts almost all lipid molecules to assemble a dense nanostructure around the nanoparticle surface. This aggression behavior also results in a loss of conformational entropy due to the confinement of lipid chains. However, in comparison with the entropic contribution to the free energy, the enthalpic contribution dominates the aggregation process, as described below.

To quantitatively reveal the physical mechanisms underlying the formation of the above-described nanostructures, we analyze the relative contributions of the three terms of the total free energy in eqn (3). The normalized values of the corresponding entropic free energy F_D of lipid molecules, the entropic free energy F_W of water molecules, and the enthalpic free energy F_E of the system are compared in Table 1. The lipid entropic free energy corresponding to a strongly charged particle (*e.g.*, $\Lambda_B = 2.75$ or 3.75) is larger than that of an uncharged or weakly charged particle (*e.g.*, $\Lambda_B = -0.75$ or 1.25). However, the enthalpic contribution to the free energy of the system containing a strongly charged particle is much lower than that for an uncharged or weakly charged particle. For instance, the difference of the lipid entropic free energy between $\Lambda_B = 3.75$ and $\Lambda_B = -0.75$ is 0.0618, whereas the corresponding enthalpic free energy has a difference of −0.3251. This demonstrates the dominant role of enthalpy in the self-assembly process of complex nanostructures surrounding a strongly charged particle.

Furthermore, we study the dependence of the self-assembled nanostructures on the particle size. Fig. 4(a–l) shows the aggregation morphologies of lipid molecules around particles of

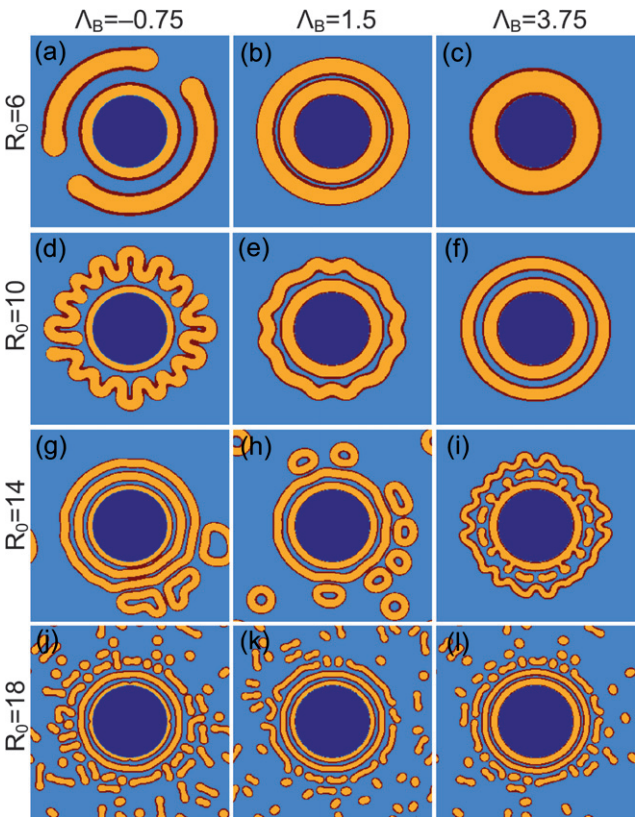

Fig. 4 Influence of the particle size R_0 on the aggregation morphologies of A-blocks (orange), B-blocks (red) and water molecules (cyan) around a nanoparticle (blue). The four rows correspond to the representative particle radii of $R_0 = 6$, 10, 14 and 18, respectively; and the three columns correspond to $\Lambda_B = -0.75$, 1.5 and 3.75, respectively.

Table 1 Comparison of the normalized free energy F of the system at equilibrium under several representative values of the charge density on the particle surface. F_D and F_W stand for the entropic contributions of lipid and water molecules to the free energy, respectively, and F_E the contribution due to enthalpic interaction. The four lines of data correspond to the self-assembled morphologies in Fig. 3(a–d), respectively

Surface charge density Λ_B	Lipid entropic contribution F_D	Water entropic contribution F_W	Enthalpic contribution F_E	Total free energy F
−0.75	0.1386	−2.2449	1.3746	−0.7317
1.25	0.1333	−2.2234	1.3524	−0.7376
2.75	0.1887	−2.1604	1.1555	−0.8163
3.75	0.2004	−2.1331	1.0495	−0.8832

several representative radii under various surface charge densities. In the simulations, the volume fraction of lipid molecules is taken as a constant $\varphi_D = 0.15$, and the volume fraction of nanoparticles is fixed as 0.11. With the increase in the particle radius R_0, the size of the calculated RVE increases in proportion but, for the sake of convenience, all the RVEs are magnified to the same size in the figures. Obviously, the self-assembled nanostructures show an evident dependence on the particle size. For uncharged particles with $\Lambda_B = -0.75$, besides the closed lipid membranes surrounding the particle, there are always a relatively large amount of free lipid molecules, which self-assemble into sphere-like, rod-like or worm-like tiny micelles or vesicles in the solution, as shown in the first column of Fig. 4. This is attributed to the relatively weak interaction between the uncharged particles and lipid molecules. For weakly charged particles with $\Lambda_B = 1.5$, the attractive interaction between the nanoparticle and lipid molecules is enhanced due to electrostatic effect. In this case, therefore, there are fewer free lipid molecules to form vesicles or micelles for small particles (Fig. 4b and e), while there still exist vesicles or micelles for larger nanoparticles (Fig. 4h and k). For strongly charged particles with $\Lambda_B = 3.75$, the electrostatic force becomes stronger and hence free vesicles or micelles only appear for the largest nanoparticles under study (Fig. 4l). The above results can be understood as follows. Since both the volume fractions of nanoparticles and lipid molecules are fixed to be constant in all the examples, the total number of lipid molecules is proportional to the square of the particle radius, while the number of lipids in a monolayer or a bilayer membrane covering a particle is approximately proportional to the particle radius. Thus, there exist more free lipid molecules to form vesicles or micelles when the particles are large. In addition, it is found that for all the particle sizes, the monolayer or bilayer lipid membranes enwrapping the nanoparticle become denser with the increase in the surface charge density. Therefore, it is concluded from Fig. 4 that the self-assembling process of lipid-nanoparticle nanostructures can be optimized by designing the size and surface charge density of nanoparticles simultaneously.

To further understand the dependence of self-assembled nanostructures on the content of lipid molecules and the particle size, a phase diagram is given in Fig. 5 summarizing the results of a number of simulations for $\Lambda_B = 1.5$. We identify six regions according to the types of lipid molecules assembly in the solution:

(i) a single bilayer (B_1), as shown in Fig. 2a;

(ii) the coexistence of a single bilayer, micelles and vesicles (B_1 + MV), as shown in Fig. 3c;

(iii) two bilayers (B_2), as shown in Fig. 4f;

(iv) the coexistence of two bilayers, micelles and vesicles (B_2 + MV), as shown in Fig. 3b;

(v) three bilayers (B_3); and

(vi) the coexistence of three bilayers, micelles and vesicles (B_3 + MV), as shown in Fig. 2e.

Such a phase diagram allows us to predict the specific nanostructures formed under given conditions. As the volume fraction φ_D of lipid molecules increases, the number of lipid layers in the concentrically layered nanostructures increases, and morphological transitions take place in the order $B_1 \rightarrow (B_1 + MV) \rightarrow B_2 \rightarrow (B_2 + MV) \rightarrow B_3 \rightarrow (B_3 + MV)$. The dependence of the nanostructures on the particles size R_0 can be clearly seen from the phase diagram.

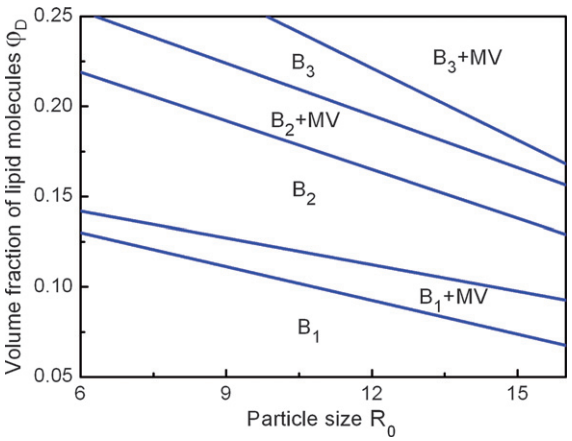

Fig. 5 A phase diagram illustrating the dependence of the self-assembled lipid nanostructures on the volume fraction of lipid molecules (φ_D) and the particle size (R_0), for the interaction parameter $\Lambda_B = 1.5$. The notations B and MV stand for lipid bilayers and micelles/vesicles, respectively, and subscripts (1,2,3) represent the number of lipid bilayers.

Conclusions

In summary, we have extended the self-consistent field method to investigate self-assembled lipid-nanoparticle nanostructures in an aqueous solution. Our simulations show that nanostructures consisting of a monolayer, a single bilayer, two or three bilayers can be formed around the nanoparticle, depending on the size and surface charge density of the nanoparticle and the concentration of lipid molecules. Some novel nanostructures have been found *via* our simulations although their biophysical properties need to be further clarified. The present method can also account for other factors (*e.g.*, shape and interaction of nanoparticles, and temperature) that may influence the self-assembly of nanostructures. This study is helpful for understanding lipid-nanoparticle interactions and for designing novel nanostructures from self-assembly of biomolecules and nanoparticles, which may have unique properties and promising applications in the field of nanomedicine. Finally, it is worth mentioning that improvements to the present calculation method will be of great interest to investigate relevant physical mechanisms in a more realistic manner.

Acknowledgements

The support from the National Natural Science Foundation of China (Grants Nos. 10732050 and 10525210) and the 973 program of MOST (2004CB619304) is acknowledged.

References

1 S. M. Moghimi, A. C. Hunter and J. C. Murray, *FASEB J.*, 2005, **19**, 311–330.
2 M. Ferrari, *Nat. Rev. Cancer*, 2005, **5**, 161–171.
3 O. C. Farokhzad and R. Langer, *Adv. Drug Delivery Rev.*, 2006, **58**, 1456–1459.
4 L. Zhang, J. M. Chan, F. X. Gu, J.-W. Rhee, A. Z. Wang, A. F. Radovic-Moreno, F. Alexis, R. Langer and O. C. Farokhzad, *ACS Nano*, 2008, **2**, 1696–1702.
5 V. Wagner, A. Dullaart, A. K. Bock and A. Zweck, *Nat. Biotechnol.*, 2006, **24**, 1211–1217.

6 V. P. Torchilin, *Nat. Rev. Drug Discovery*, 2005, **4**, 145–160.
7 L. Zhang and S. Granick, *Nano Lett.*, 2006, **6**, 694–698.
8 N. Nasongkla, E. Bey, J. Ren, H. Ai, C. Khemtong, J. S. Guthi, S.-F. Chin, A. D. Sherry, D. A. Boothman and J. Gao, *Nano Lett.*, 2006, **6**, 2427–2430.
9 H. Otsuka, Y. Nagasaki and K. Kataoka, *Adv. Drug Delivery Rev.*, 2003, **55**, 403–419.
10 H. Ai, C. Flask, B. Weinberg, X. Shuai, M. D. Pagel, D. Farrell, J. Duerk and J. Gao, *Adv. Mater.*, 2005, **17**, 1949–1952.
11 N. R. Soman, G. M. Lanza, J. M. Heuser, P. H. Schlesinger and S. A. Wickline, *Nano Lett.*, 2008, **8**, 1131–1136.
12 S. Sengupta, D. Eavarone, I. Capila, G. Zhao, N. Watson, T. Kiziltepe and R. Sasisekharan, *Nature*, 2005, **436**, 568–572.
13 A. Bershteyn, J. Chaparro, R. Yau, M. Kim, E. Reinherz, L. Ferreira-Moita and D. J. Irvine, *Soft Matter*, 2008, **4**, 1787–1791.
14 I. De Miguel, L. Imbertie, V. Rieumajou, M. Major, R. Kravtzoff and D. Betbeder, *Pharm. Res.*, 2000, **17**, 817–824.
15 A. M. Carmona-Ribeiro, *Chem. Soc. Rev.*, 2001, **30**, 241–247.
16 J. Thevenot, A.-L. Troutier, J.-L. Putaux, T. Delair and C. Ladavière, *J. Phys. Chem. B*, 2008, **112**, 13812–13822.
17 K. A. Smith, D. Jasnow and A. C. Balazs, *J. Chem. Phys.*, 2007, **127**, 084703.
18 H. Gao, W. Shi and L. B. Freund, *Proc. Natl. Acad. Sci. U. S. A.*, 2005, **102**, 9469–9474.
19 V. V. Ginzburg and S. Balijepalli, *Nano Lett.*, 2007, **7**, 3716–3722.
20 M. W. Matsen, *J. Phys.: Condens. Matter*, 2002, **14**, R21–R47.
21 F. Schmid, *J. Phys.: Condens. Matter*, 1998, **10**, 8105–8138.
22 X. He, H. Liang, L. Huang and C. Pan, *J. Phys. Chem. B*, 2004, **108**, 1731–1735.
23 R. Wang, Z. Jiang, Y.-L. Chen and G. Xue, *J. Phys. Chem. B*, 2006, **110**, 22726–22731.
24 F. Drolet and G. H. Fredrickson, *Phys. Rev. Lett.*, 1999, **83**, 4317–4320.
25 F. Drolet and G. H. Fredrickson, *Macromolecules*, 2001, **34**, 5317–5324.
26 M. W. Matsen, *J. Chem. Phys.*, 1997, **106**, 7781–7791.
27 J. Y. Lee, Z. Shou and A. C. Balazs, *Phys. Rev. Lett.*, 2003, **91**, 136103.
28 R. B. Thompson, V. V. Ginzburg, M. W. Matsen and A. C. Balazs, *Science*, 2001, **292**, 2469–2472.
29 G. Tzeremes, K. Ø. Rasmussen, T. Lookman and A. Saxena, *Phys. Rev. E*, 2002, **65**, 041806.
30 S. W. Sides and G. H. Fredrickson, *Polymer*, 2003, **44**, 5859–5866.
31 X. Qiu, S. Leporatti, E. Donath and H. Möhwald, *Langmuir*, 2001, **17**, 5375–5380.
32 Z. An, G. Lu, H. Möhwald and J. Li, *Chem. Eur. J.*, 2004, **10**, 5848–5852.
33 J. Li, H. Möhwald, Z. An and G. Lu, *Soft Matter*, 2005, **1**, 259–264.
34 M. J. Fasolka and A. M. Mayes, *Annu. Rev. Mater. Res.*, 2001, **31**, 323–355.